

DESIGN INFLUENCED BY THE EFFECT OF FILTER SELECTION ON THE APPRAISER VARIATION OF THE MEASURING RESULTS OF A 3D OPTICAL MEASURING SYSTEM

ZASNOVA, KI VPLIVA NA IZBIRO FILTRA ZA OCENO MERILNIH REZULTATOV 3D OPTIČNEGA MERILNEGA SISTEMA

Josip Groš², Tihomir Mihalić^{2*}, Srđan Medić³, Nikola Šimunić⁴

Keywords: 3D optical measuring systems, Gaussian best fit, Chebyshev best-fit, Minimum circumscribed element and Maximum inscribed element

Abstract

During the previous decade, 3D optical measuring systems have had an increasing application regarding quality control in different industrial branches where they are commonly used to monitor parts made from sheets, polymers, and castings. The biggest disadvantage of 3D measuring devices is the lack of ISO standards for the calibration of such devices, making it difficult to estimate the quality of the measuring results. The introductory part of the present paper elaborates the working principle of the 3D optical measuring system. In this paper, the free software package GOM inspect is used. When marking the geometric features of the measured metering object, GOM inspects different filters for the selection of the aforementioned features. The experimental part of the paper elaborates the influence of usage of different filters (Gaussian best fit, Chebyshev best-fit, Minimum circumscribed element and Maximum inscribed element) on the measuring results. Reference results are measurements performed on a device with a higher level of accuracy (coordinate measuring device). Afterwards, a comparison of the reference results and measures performed with 3D optical measuring systems using different filters was made.

¹ Corresponding author: Tihomir Mihalić, PhD., University of Applied Sciences, Karlovac, Tel.: +385 98 686 072, Mailing address: I.Meštrovića 10, Karlovac, Croatia E-mail address: tihomir.mihalic@vuka.hr

Povzetek

V zadnjem desetletju imajo 3D optični merilni sistemi vse večji pomen pri nadzoru kakovosti v različnih industrijskih panogah, kjer se pogosto uporabljajo za nadzor delov iz pločevine, polimerov in ulitkov. Največja pomanjkljivost 3D merilnih naprav je pomanjkanje ISO standardov za kalibracijo 3D optičnih merilnih naprav, kar otežuje oceno kakovosti merilnih rezultatov. V uvodnem delu prispevka je predstavljeno načelo dela 3D optičnega merilnega sistema. V tem prispevku je za analizo uporabljen brezplačni programski paket GOM inspect. Med označevanjem geometrijskih značilnosti merjenega merilnega predmeta GOM pregled ponuja različne filtre za izbiro zgoraj omenjenih lastnosti. Eksperimentalni del prispevka pojasnjuje vpliv uporabe različnih filtrov na rezultate meritev. Referenčni rezultati so meritve, opravljene na napravi z višjo stopnjo natančnosti (koordinatna merilna naprava). V članku je bila narejena tudi primerjava referenčnih rezultatov in meritev, izvedenih s 3D optičnimi merilnimi sistemi z uporabo različnih filtrov.

1 INTRODUCTION

The 3D optical measuring method is a non-contact metering method. Its field of application is very wide and includes everything from quality control to archaeology, the auto industry, aeronautics, and even medicine.

Metering systems that use optical measuring methods to display an object are called “3D optical measuring systems”. Originally, they were used only for reverse engineering, but nowadays they are widely used in measuring and product quality control.

In production engineering, there is a growing need for fast and precise measuring of geometric characteristics, resulting from increasing demands for quality, thanks to the ever-growing competition and production automatization.

The development of new products increased their complexity regarding their geometric characteristics. They are becoming increasingly elaborate in order to decrease the total number of parts in production while requirements for their functionality simultaneously increase. Previous production methods were relatively restrictive regarding the complexity of the design resulting in the simplicity of lines and shapes of the final product. Such products had relatively simple demands regarding quality control.

However, nowadays, in addition to the precision of manufacturing, great attention is given to the speed of product development, resulting in an increasing need for new approaches regarding measuring and controlling the geometry of the shape. That is why quality control is now present as early as manufacturing certain parts of the final product or immediately after that, opposed to previous quality control of the finished product at the end of the production process.

Due to the constant progress of the industry, the production boundaries change more rapidly, as more elaborate and complex items are being made, resulting in increasing demands

regarding the accuracy of production as well as allowed tolerances. Therefore, the measuring devices need to adopt imposing trends regarding high speed and accuracy of measurement.

1.1 Mathematical model of triangulation [1]

The camera and projector are based on a model of the same perspective of projection with radial and tangential lens distortions maximum to the 4th order. As shown in Figure 5., $P_w = [X Y Z]^T$ is a point within a coordinate system of real space (0-XYZ) with coordinates within the coordinate system of the device (0-xyz) formulated by $P = [x y z]^T$. This transformation of the solid object from P_w onto P can be expressed through Equation 1, in which R and T are rotational (i.e., translational) matrices.

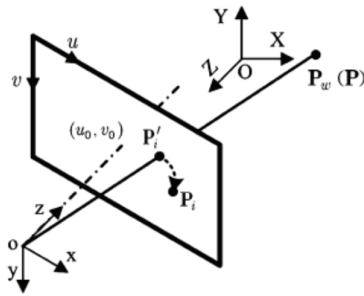


Figure 1: Triangulation method

$$P = RP_w + T \tag{1}$$

Let us say that P_n is a projection of the point P onto a normalized representative plane, which is parallel with the representative plane and positioned at a unit distance from the centre of the lens 0. In that case, P_n can be expressed through Equation 2.

$$P_n = \begin{bmatrix} x_n \\ y_n \end{bmatrix} = \begin{bmatrix} \frac{x}{z} \\ \frac{y}{z} \end{bmatrix} \tag{2}$$

Taking into consideration the influence of radial and tangential distortions of the lens onto P_n , we have a distorted projection of the P_d on the normalized representative plane derived through equation 3., in which $r^2 = x_n^2 + y_n^2$ and $K = [k_1 k_2 k_3 k_4]$ is a lens distortion coefficient.

$$P_d = f_d(P_n, K) = \begin{bmatrix} x_d \\ y_d \end{bmatrix} = P_n + (k_1 r^2 + k_2 r^4)P_n + \begin{bmatrix} 2k_3 x_n y_n + k_4 (r^2 + 2x_n^2) \\ k_3 (r^2 + 2y_n^2) + 2k_4 x_n y_n \end{bmatrix} \tag{3}$$

The last two elements of Equation 3 represent the radial and tangential distortions of the lens. In that case, the projection on the representative plane P_i can be expressed as shown in Equation 4, in which f_u and f_v represent the horizontal and vertical focal lengths, while u_0 and v_0 present the coordinates of the principal point.

$$P_i = \begin{bmatrix} u \\ v \end{bmatrix} = \begin{bmatrix} f_u x_d + u_0 \\ f_v y_d + v_0 \end{bmatrix} \quad (4)$$

In summary, the camera and the projector model can be described according to Equation 5., in which function g describes the imaging from the actual coordinate system onto a representative plane, while $\Theta = [R \ T \ f_u \ f_v \ u_0 \ v_0 \ K]$ represents the model parameter.

$$P_i = g(P_w, \Theta) \quad (5)$$

2 FILTERS FOR THE SELECTION OF THE CONTROL ELEMENTS

Depending on the desired object of construction, four methods can be used. Each of them has its advantages and disadvantages, and each is used depending on the object of the measurement. The Gauss filter uses normal distribution and eliminates the furthest points during the calculation. The number of points used for the calculation can be determined by changing the sigma value. The Chebyshev filter is used for GD&T (tolerance of the position and shape). The norm prescribes that the element must be defined through that method in case of verifying tolerance of the position and the shape of the element.

It might be easiest to explain the usage of the remaining two filters through their practical application. The maximum inscribed element filter should be used in cases of, for example, defining the maximum axle diameter, while the minimum circumscribed element filter would be used for defining the minimum diameter of the hole.

2.1 The Gaussian best-fit filter

The filter is based on the calculation in which the total square deviations from the given points are smallest. Figure 2. shows the possibility of selecting the so-called "Used Points". That function is active only in the limits of this method. Using statistical methods, it is possible to eliminate points that are located outside the model but are included in the selected area.

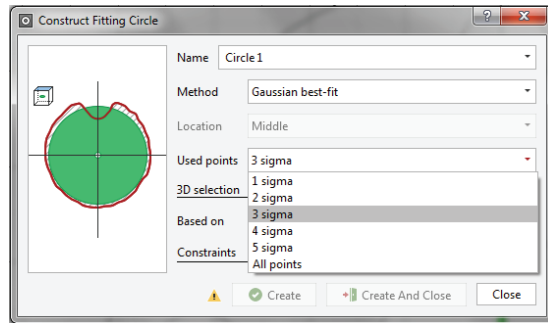


Figure 2: The Gaussian best-fit filter [2]

The method is calculated so that the maximum distance of all selected points or polygons on the constructed element is minimal. Unlike the Gauss principle, Chebyshev's best-fit filter always takes into consideration the furthest points of the selected area.

When selecting a filter, it is also possible to define the application area itself, i.e. the location (positioning) to which the method applies (Figure 3).

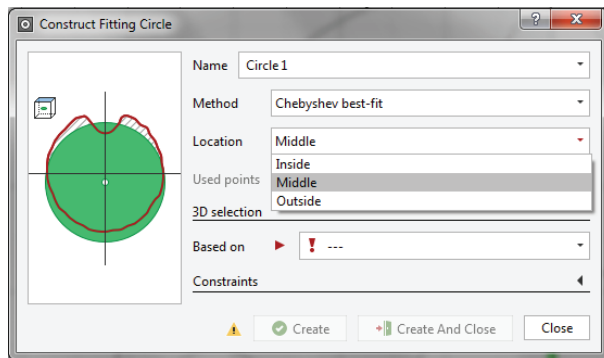


Figure 3: The Chebyshev best-fit filter [2]

The comparison of those locations is shown on Figure 4., on which a) presents area included in location selection "inside", b) presents location selection "middle", while c) presents location selection "outside".

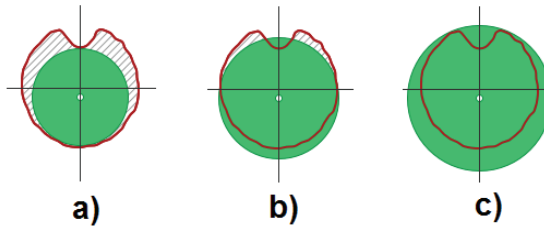


Figure 4: Review of the area covered by location selection, [2]

Figure 5 shows all locations on the same model. It can be easily seen that all locations have a common centre.

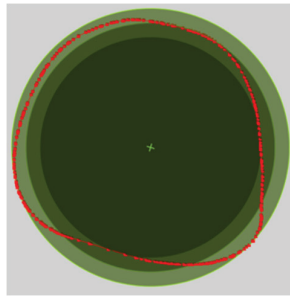


Figure 5: Comparison of all locations on the same model, [2]

2.2 Maximum inscribed element

Using this filter, we obtain the largest possible element that is positioned inside the selected points or polygons.

Figure 6. shows the area (marked green) which is obtained by this filter while the red curve shows the selected area.

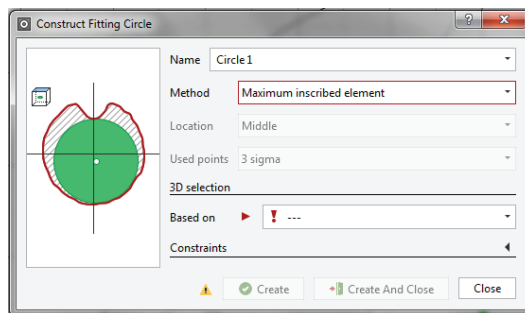


Figure 6: Maximum inscribed element filter, [2]

2.3 Minimum circumscribed element

Using this filter, we obtain the smallest possible element that includes selected points or polygons.

Figure 7. shows the area which is obtained by this filter (marked green) in relation to selected points (red curve).

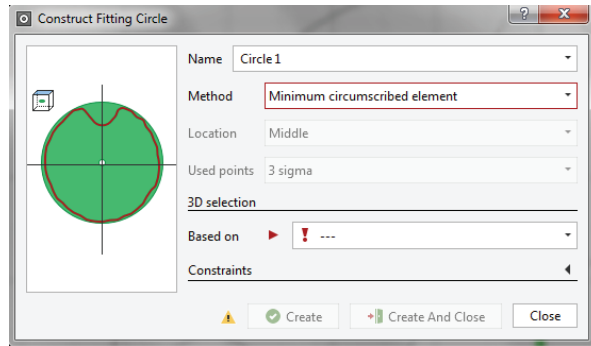


Figure 7: Minimum circumscribed element filter [2]

3 EXPERIMENTAL PART OF THE MEASUREMENT OF THE HOLE ON THE FLANGE

In the experimental part of the paper regarding reproducibility of the measuring results obtained by a 3D optical measuring devices, the measuring system provided by the company Steinbichler COMET 1.4, which includes an automated turntable, is used.

The measuring device uses a structured light by which it decreases the influence of the external light on the measuring result, [3][4]. The flange was measured with the use of an automated turntable and without referent points. 3D optical measuring systems have certain limitations regarding the measurement of the geometric and dimensional features of reflective and transparent surfaces, [5][6][7]. Due to the reflective surfaces, white powder spray was used during the measurement process. Not using such a spray causes mistakes in the measurement process [2].

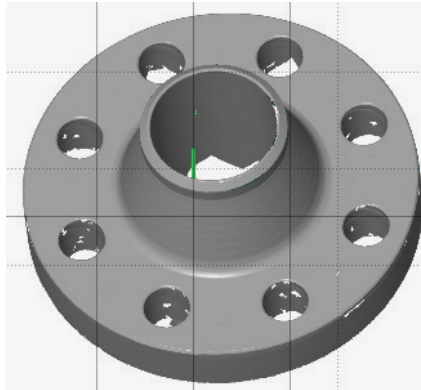


Figure 8: Layout of the 3D stl model

Figure 8. shows the 3D model that has a total of 396,168 measured points; it was obtained by capturing from 6 different positions. Any mistakes are eliminated from the model via mesh as an auxiliary to define the orientation: three-dimensional cylinders and a plane were also constructed using the Gaussian best fit method (Figure 9) and 3 sigma (the percentage of used points out of the total number of selected points).

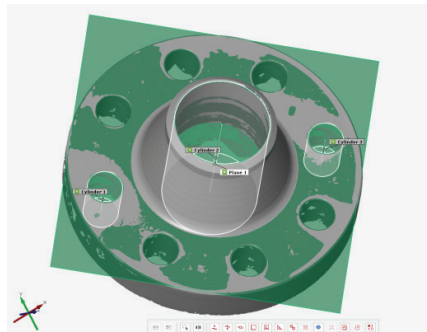


Figure 9: Construction of the cylinder and the plane

The model was oriented by the means of the 3-2-1 method. After orientation, two cross-sections were constructed, one of which is distanced from the plane z for 5 mm in the negative direction while the other one is distanced for 30 mm in the positive direction.

Figure 10 shows the construction of the cross-section and the circularly distributed bores, and both will be controlled for the purpose of confirming the reproducibility of measuring result.

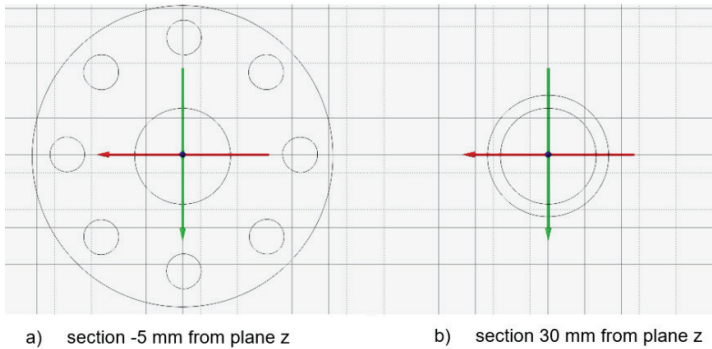


Figure 10: Construction of the cross-section

The next step is the construction of the circulars, followed by the measurement of the same. Using the model, a total of 11 measurements was made, and all filters have been used. All 11 diameters were measured, and a standard deviation was calculated as described in the following chapter.

3.1. Calculation of the standard deviation

Standard deviation presents the numerical evaluation of the accuracy of the measuring procedure. When it is smaller, the precision of the measurement is greater. Precision or imprecision is not the same as “inaccuracy”, which shows the correlation between the result of the measurement and the true value of the measuring size, [8].

With the help of the standard deviation, it is simple to apply a 3 s test, which is used on a set of data that behaves according to normal distribution. It is a statistical test on which we base the criteria for determining a gross error. A gross error of a measurer arises from different reasons, such as measurer negligence, application of inadequate measuring equipment or inadequate measuring instrument, reading the results on the wrong scale or reading the wrong value, omitting the digit when reading the scale, etc., [9].

Equation 7 was used to calculate the standard deviation follows:

$$s = \sqrt{\frac{\sum_{i=1}^n (x_i - \bar{x})^2}{n-1}} \quad (6)$$

$$\bar{x} = \frac{x_1 + \dots + x_n}{n} = \frac{\sum_{i=1}^n x_i}{n} \quad (7)$$

x_i ...measuring results

\bar{x} ...arithmetic average of measuring results

s... approximate standard deviation

3.2. Results of measuring the 11 holes

The results of measuring the 11 holes in 6 different positions can be seen in Table 1. With different filters, the measuring results of the hole vary significantly. The results of the measuring are compared to the results of the measuring obtained by a coordinate measuring device (marked as reference measures in Table 1).

Table 1: Results of measuring the 11 holes in 6 different positions

DIAMETER P6												
Number of diameter	GAUSSIAN BEST-FIT (1 SIGMA)	GAUSSIAN BEST-FIT (2 SIGMA)	GAUSSIAN BEST-FIT (3 SIGMA)	GAUSSIAN BEST-FIT (4 SIGMA)	GAUSSIAN BEST-FIT (5 SIGMA)	GAUSSIAN BEST-FIT (ALL POINTS)	CHEBYSHEV BEST-FIT (INSIDE)	CHEBYSHEV BEST-FIT (MIDDLE)	CHEBYSHEV BEST-FIT (OUTSIDE)	MAXIMUM INSCRIBED ELEMENT	MINIMUM CIRCUMSCRIBED ELEMENT	The reference measurement (CMM)
1	19,0262	19,0377	19,0377	19,0377	19,0377	19,0377	18,9041	19,0553	19,2065	18,9163	19,1923	19,137
2	19,1602	19,1796	19,1796	19,1796	19,1796	19,1796	19,0374	19,2124	19,3875	19,0403	19,3574	19,216
3	19,0714	19,0708	19,0747	19,0747	19,0747	19,0747	19,0012	19,0678	19,1343	19,0254	19,1331	19,099
4	19,1411	19,1498	19,1498	19,1498	19,1498	19,1498	18,9845	19,1683	19,352	18,9931	19,3465	19,178
5	19,2274	19,2303	19,2303	19,2303	19,2303	19,2303	19,0343	19,2489	19,4635	19,0459	19,4424	19,253
6	19,0772	19,0795	19,0795	19,0795	19,0795	19,0795	18,943	19,0783	19,2136	18,9568	19,2104	19,133
7	19,064	19,0592	19,0658	19,0658	19,0658	19,0658	18,9385	19,0716	19,2047	18,9665	19,1872	19,12
8	19,1097	19,1211	19,1242	19,1242	19,1242	19,1242	18,996	19,1696	19,3433	19,0007	19,286	19,18
9	52,4915	52,4913	52,4911	52,4911	52,4911	52,4911	52,4765	52,4893	52,502	52,4785	52,502	52,48
10	164,7637	164,7645	164,7672	164,768	164,768	164,768	164,7355	164,7793	164,8231	164,7399	164,823	164,769
11	52,4613	52,46	52,46	52,46	52,46	52,46	52,4391	52,459	52,4789	52,4391	52,4783	52,503

Figure 11 shows the usage of the filters on 11 holes. Each method is marked with a colour, and the diagram shows not only methods but also the curve of the referent measurement. The curves are distributed into three groups, which can provide insight to which of the methods used are more similar, resulting in similar final results, i.e., which methods calculate the data similarly.

Two curves that stand out with the highest values are the one obtained by using a Chebyshe’s best-fit (outside) and Minimum circumscribed element methods. Two curves that have the lowest values are obtained by using a Chebyshe’s best-fit (inside) and Maximum inscribed element methods.

At the middle of the diagram, we observe the curves which refer to that Gaussian method and its combinations as well as the curves obtained by Chebyshe’s best-fit (middle) method and the curve of referent measurement.

If we examine that set of curves, it is seen that the curves obtained with the Gaussian method almost all overlap, while those obtained with 1 sigma and 2 sigma stand out from the set and the ones obtained by 3 and more sigma, including the one that contains all selected points, also overlap. The reason for such a result is that starting from 3 sigma the method uses a 99.7% of the total number of the selected points.

Chebyshe’s best-fit (middle) curve, and, consequently, the results used to create the curve are the middle value of the Chebyshe’s best-fit (inside) and Chebyshe’s best-fit (outside) method. The results obtained by this method, and consequently the layout of the curve, show that in several places they overlap with the results obtained with the referent measurement while sometimes they overlap with the results obtained with Gaussian best-fit methods.

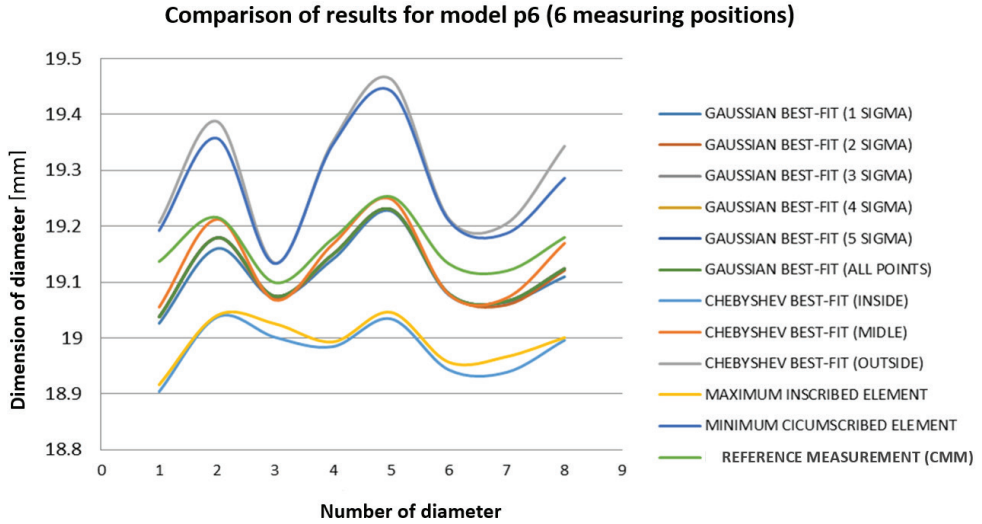


Figure 11: Use of different filters for 6 measurement positions

Every measurement was repeated five times in the shortest possible time range. The calculation of the standard deviation is given in Table 3. All the filters previously explained were used.

Table 3: Standard deviation results for 11 holes

Number of diameter	STANDARD DEVIATION RESULTS											
	Filters											
	Gaussian 1 sigma	Gaussian 2 sigma	Gaussian 3 sigma	Gaussian 4 sigma	Gaussian 5 sigma	Gaussian all points	Chebyshev best fit (inside)	Chebyshev best fit (middle)	Chebyshev best fit (outside)	Maximum inscribed element	Minimum circumscribed element	CMM
1	0,004084	0,001481	0,001481	0,001481	0,001481	0,001481	0,00127	0,002391	0,005269	0,003005	0,003456	0,003564
2	0,00349	0,000626	0,000626	0,000626	0,000626	0,000626	0,006276	0,002285	0,004957	0,00188	0,004245	0,002702
3	0,001128	0,000687	0,000907	0,000862	0,000862	0,000862	0,002411	0,002975	0,006829	0,000728	0,006683	0,002236
4	0,001322	0,001834	0,001834	0,001834	0,001834	0,001834	0,004034	0,002121	0,001218	0,004908	0,001689	0,002387
5	0,006214	0,00334	0,002639	0,002639	0,002639	0,002639	0,01104	0,005551	0,008901	0,005024	0,01073	0,001924
6	0,005633	0,002612	0,002612	0,002612	0,002612	0,002612	0,002119	0,001885	0,002228	0,002017	0,001725	0,002074
7	0,002382	0,00235	0,002277	0,002277	0,002277	0,002277	0,003564	0,003462	0,003803	0,00232	0,001288	0,001581
8	0,00703	0,003992	0,002442	0,002442	0,002442	0,002442	0,006776	0,003316	0,002581	0,004296	0,003749	0,001924
9	0,001323	0,001067	0,001016	0,001013	0,001013	0,001013	0,001751	0,001681	0,002963	0,001784	0,002382	0,001920
10	0,001235	0,000377	0,000606	0,000644	0,000644	0,000644	0,003963	0,003848	0,004531	0,002245	0,004489	0,00158
11	0,001473	0,001438	0,00142	0,00142	0,00142	0,00142	0,001355	0,001159	0,001212	0,001332	0,001094	0,00192

Diagram analysis makes it easy to conclude that usage of any filter (Gauss, Cheyshes best fit and others) regarding control of the hole will not give a satisfying comparable result.

Of the four main filters (i.e. a total of 11 possible combinations regarding control of the hole), at first glance four of them strongly stand out with their results in comparison to referent values obtained by a coordinate measuring device and to which they are compared.

Of these four, two whose values were significantly lower than the required ones are Maximum inscribed element and Chebyshev's best fit (inside) due to the method they use to analyze the selected data. Figure 4a and Figure 6 show the selected area in relation to the total selected area that those filters take into consideration during calculation. Therefore, the obtained values are lower, so we can conclude that these methods are not suitable for such type of measurement. The other two filters whose values were significantly higher than the required ones are Minimum circumscribed element and Chebyshev's best fit (outside).

Unlike the Maximum inscribed element and Chebyshev's best fit (inside), the methods mentioned above during calculation take into consideration an area that is larger than the selected area. This is best seen in Figure 4c and Figure 7. Therefore, these filters are also not suitable for such type of measurement. Comparing the other seven filters (all Gaussian best fit and Chebyshev's best fit (middle)) with the referent values obtained by a coordinate measuring device, it is noticeable that, unlike the filters mentioned above, the given results are much closer to the required values, (i.e. the compared values). By defining one of the sigma, the Gaussian best fit filter defines the percentage of points taken into consideration during the calculation, in relation to the total number of selected points, which allows the elimination of points that are located outside of the model but are inside of the selected area. With all point options, all selected points are taken into the calculation. As the percentages range starting from 68.3% for sigma 1 to higher values, the curves obtained with Gaussian best-fit filters are similar in appearance and the results obtained with 3 sigma (or more) are almost identical, resulting in an almost identical appearance of their curves. Chebyshev's best fit (middle) is obtained as an average value of Chebyshev's best fit (inside) and Chebyshev's best fit (outside). The area taken into consideration for the calculation is best seen in Figure 4.b. By comparing the curves (Gaussian best fit, Chebyshev best fit (middle)) by the points that represent the number of holes measured by referent values, it is noticeable that holes 2, 4, 5 and 8 obtained by Chebyshev's best fit (middle) filter almost overlap with the referent values, while that is not the case with the Gaussian best fit filter. The curve obtained by Chebyshev's best fit (middle) filter has much more expressed specified amplitudes, i.e., on the specified holes the results almost overlap, while on others they stand out quite a bit from the required values. The Gaussian best-fit curves follow in appearance the curve obtained by the referent values, but in relation to it, they have results showing somewhat lower values. That can be a result of measurement performed by a measuring device with a lower level of accuracy compared to the coordinate measuring device. Whereas each measurement was repeated five times, by calculating the standard deviation we can determine the precision of the measuring procedure. When the deviation is smaller (i.e. the lower the given number is), the precision of the measurement is greater. By the means of such control, it is easiest to eliminate the gross errors, because the obtained results will significantly deviate from the other results. The calculation of standard deviation was calculated for each hole separately (Table 3), and each measurement was repeated five times; consequently, values of each of the five measurements of the hole (marked with numbers ranging from 1 to 11) have been compared. It is noticeable that the majority of the filters have the same deviation up to

the third decimal place, compared to calculated standard deviation of the results obtained with a coordinate measuring device.

4 SUMMARY

From day to day, technology is progressing more and more, new possibilities of production of more complicated and more complex products with high demands regarding quality, functionality and mere aesthetics are being offered. 3D optical measuring systems are increasingly being implemented in manufacturing processes even though they lack ISO calibration standards. Currently, there are VDI / VDE 2634 recommendations, but a relationship with the national metering standard has not established.

The purpose of this paper is to stimulate thinking regarding the necessity of setting standards for calibration of 3D optical metering systems, not only in the scientific community but also regarding all those who use 3D optical measuring systems.

This paper showed a great lack of uniformity regarding the results since the measurement results can easily be changed using a filter, which produces a non-uniform result.

For a long time, authors have used 3D optical measuring systems for measuring machine parts for the purpose of quality control. The stl files obtained after measuring show great disadvantages regarding their usage, for instance, the original measuring result can be easily changed and refined (mesh: smooth, thin, refine and repair).

Improvements are possible in the development of a new stl file that could not be changed (i.e., measuring stl file). With each result using a particular filter, a note should be added to allow the ordering client to be sure which filter was used. That would ensure a more credible measuring report.

This is one of the presuppositions for the development of ISO norms for the calibration of the 3D optical measuring systems. According to the research, the class of accuracy of the 3d optical measurement systems is 0.1 mm.

References

- [1] **Croatian Standards Institute:** *HRN EN ISO/IEC 17025:2007*
- [2] **Zeiss group:** *User manual GOM Inspect Direct Help, V7 SR2*
- [3] **C. Bernal, B. de Agustina, M.M. Marín, A.M. Camacho:** *Performance evaluation of optical scanner based on blue LED Structured light*, *Procedia Engineering*, Vol. 63, 591–598, 2013
- [4] **K. Xue, V. Kurella, A. Spence:** *Multi-sensor blue LED and touch probe inspection system*, *Computer-Aided Design and Applications*, 2016,

- 5] **M.A.B. Ebrahim:** *3D Laser Scanners' Techniques Overview*, International Journal of Science and Research, Volume 4, Issue 10, 2015
- 6] **S. Gerbino, D.M.D. Giudice, G. Staiano, A. Lanzotti, M. Martorelli:** *On the influence of scanning factors on the laser scanner-based 3D inspection process*, Int J Adv Manuf Technol, 2016, 84, 1787
- 7] **B. Boeckmans, M. Zhang, F. Welkenhuyzen, J. P. Kruth:** *Determination of Aspect Ratio Limitations, Accuracy and Repeatability of a Laser Line Scanning CMM Probe*, International Journal of Automation and Control Technology Vol.9 No.5, 2015
- 8] <http://racunala.ttf.unizg.hr/files/Statistika.pdf>
- 9] **B. Runje:** *Predavanja iz kolegija teorija i tehnika mjerenja*, FSB Zagreb, 2014